Article

Discovery Medicine 2026; 38(208): 1417–1433
https://doi.org/10.24976/Discov.Med.202638208.111

Identification of Circadian Rhythm-Related Genes in Preeclampsia by RNA-seq and Integrative Bioinformatics Analysis

Yuqing Xiang[1], Tianxin Zhang[1], Xia Ma[1], Jie Li[1], Min Jin[1], Xiaoxiao Jin[1,*], Feng Qi[1,*]

[1]Department of Obstetrics and Gynecology, Taizhou Hospital of Zhejiang Province, 317000 Taizhou, Zhejiang, China
*Correspondence: jxx5662819@outlook.com (Xiaoxiao Jin); qif@enzemed.com (Feng Qi)
Submitted: 5 December 2025 Revised: 25 February 2026 Accepted: 30 March 2026 Published: 20 May 2026

Background: Preeclampsia (PE) is a serious pregnancy-related disorder with incompletely understood etiology. The occurrence and development of preeclampsia are closely related to multiple biological regulatory mechanisms, among which circadian rhythm disorders are believed to possibly play an important role in abnormal placental function and immune imbalance. However, systematic research on the expression characteristics of circadian rhythm-related genes in preeclampsia and their potential diagnostic value remains scarce. This study aims to systematically identify the circadian rhythm genes associated with preeclampsia using placental RNA sequencing data, and to evaluate their biological functions and clinical diagnostic potential through comprehensive bioinformatics analysis.

Methods: Placental tissues from 5 PE patients and 6 matched controls were subjected to RNA sequencing. Bioinformatics processing included normalization and differential expression analysis using the limma package, batch-effect correction assessed via principal component analysis (PCA), and identification of circadian rhythm-related differentially expressed genes (CRRDEGs) through Venn analysis. Their expression patterns were displayed with heatmaps. Diagnostic performance was evaluated by generating receiver operating characteristic (ROC) curves and calculating area under the curve (AUC) values using the pROC package. Further functional characterization was conducted via Gene Set Enrichment Analysis (GSEA) and Gene Ontology (GO) enrichment, supported by protein–protein interaction (PPI), mRNA–miRNA, mRNA–transcription factor (TF), and mRNA–drug network analyses. Immune infiltration was examined with ssGSEA and CIBERSORT algorithms.

Results: We identified 373 differentially expressed genes (DEGs), including five CRRDEGs (*MTTP*, *PROK1*, *UTS2*, *NKX2-1*, and *PRKAA2*). Among them, *PROK1* and *NKX2-1* demonstrated high diagnostic accuracy (AUC $\geq$0.9). GSEA indicated significant enrichment in autophagy, autoimmune thyroid disease, transcriptional activity, and ribosomal pathways. GO analysis highlighted involvement in circadian regulation, calcium response, and lipid homeostasis. Integrated network analysis suggested relevant miRNAs, TFs, and drugs as potential therapeutic targets. Immune infiltration assessment revealed four immune cell subsets with significantly altered abundance in PE.

Conclusions: This study elucidates the role of circadian rhythm-related genes in the pathogenesis of PE and identifies candidate biomarkers and therapeutic targets. Further validation in expanded cohorts and clinical studies is necessary to translate these findings into early diagnostic and interventional strategies.

Keywords: biomarkers; circadian rhythms; differential expression; immune infiltration; ROC curve

Introduction

Preeclampsia (PE) is a systemic condition characterized by the emergence of hypertension and end-organ dysfunction occurring after 20 weeks of gestation. It may result in serious complications such as uncontrolled hypertension, hypertensive encephalopathy, stroke, eclampsia, heart failure, pulmonary edema, HELLP syndrome, disseminated intravascular coagulation, placental abruption, and intrauterine fetal death. In recent years, the global incidence of PE has shown a declining trend. Nevertheless, it remains a major contributor to maternal and fetal mortality across diverse geographical regions. As stated in a report by Laura A. Magee *et al.* [1] published in The New England Journal of Medicine, PE is responsible for more than 46,000 maternal deaths and approximately 500,000 perinatal deaths annually worldwide, accounting for 4.7% to 41.6% of maternal mortality causes, with the highest burden observed in low- and middle-income countries [2]. Reports from different countries indicate that the incidence of severe complications of PE varies but remains consistently high. These complications can occur simultaneously or sequentially, resulting in serious adverse outcomes. Consequently, PE continues to be a major contributor to maternal and fetal mortality across diverse geographical regions. However, the mechanisms underlying PE are not well understood, and

the diagnostic criteria rely primarily on clinical features that typically manifest in the later stages of the disease [3]. This highlights the urgent need for identifying early biomarkers to predict PE and potentially guide preventive strategies.

The biological processes modulated by circadian rhythm genes—encompassing hormonal regulation, immune response, and cellular proliferation—are critically involved in the pathophysiology of PE [4,5]. Circadian rhythm disturbances correlate with unfavorable pregnancy outcomes. In a notable study by Aïssatou Bailo Diallo *et al*. [6], placental macrophages were shown to exhibit pronounced circadian expression patterns, offering the first evidence of intrinsic rhythmicity and melatonin synthesis in this cell population. These findings reveal that preeclampsia is related to the disruptions in the circadian rhythm of placental cells. Furthermore, Carlos Venegas and colleagues [7] confirmed that melatonin treatment inhibited the circadian oscillations of *BMAL1*, *PER2* and *WEE1* in placental tissue [6]. However, their exact contribution to PE pathogenesis requires further investigation. Research on circadian-associated pathologies has shown that circadian rhythm-related genes (CRRGs) may serve as potential biomarkers and therapeutic candidates, indicating that comparable methodologies might aid in deciphering and managing this disorder [4].

According to this study, gene expression of PE was analyzed using bioinformatics approaches to determine whether it exhibits circadian rhythmicity. However, their precise contribution to the pathogenesis of PE remains to be further investigated. Intersections with CRRGs obtained from PubMed were visualized using Venn diagrams and heatmaps. Diagnostic potential was assessed via receiver operating characteristic (ROC) curves with calculation of area under the curve (AUC) values. Gene Set Enrichment Analysis (GSEA) and Gene Ontology (GO) provided insights into the biological functions of the genes. Protein–protein interaction (PPI) networks were constructed along with mRNA-miRNA, mRNA-TF, and mRNA-drug interaction networks. Immune cell infiltration was analyzed using ssGSEA and CIBERSORT algorithms.

Our findings revealed significant differences in circadian rhythm-related differential gene expression between PE samples and controls. ROC analysis confirmed the diagnostic utility of these genes, with AUC values reflecting their accuracy. GSEA and GO suggested that these genes may regulate biological pathways. Through network analysis, we gained new insights into the pathogenic functions of these genes in PE and their potential as therapeutic targets. Correspondingly, immune profiling demonstrated that variations in immune cell composition within PE tissues were significantly associated with the expression patterns of the identified genes.

This study provides a pioneering framework for elucidating the molecular mechanisms underlying PE using circadian biology. Our results pave the way for future research on early diagnostic biomarkers and potential therapeutic interventions aimed at modulating circadian rhythms to improve pregnancy outcomes.

Methods

Data Acquisition and Preprocessing

In this study, all samples from the PE and control groups consisted of placental tissue collected from pregnant women at the Taizhou Hospital of Zhejiang Province, and no different cell types were isolated. Using pregnant women who underwent cesarean section at full term due to a scarred uterus as the control group, and pregnant women who underwent cesarean section at full term and met the diagnostic criteria for preeclampsia as the experimental group. Inclusion criteria: Full-term singleton pregnant women aged 18 to 49 who meet the diagnostic criteria for preeclampsia; Exclusion criteria: ① Concurrent pregnancy complications and comorbidities; ② Conception through assisted reproductive technology; ③ History of chronic diseases and long-term medication. During the procedure, a portion of placental tissue was excised, rinsed with 0.9% normal saline to remove blood, and immediately stored in a –80 °C freezer. Total RNA was isolated and purified using TRIzol reagent (Invitrogen, Carlsbad, CA, USA) following the manufacturer's procedure. The RNA amount and purity of each sample were quantified using NanoDrop ND-1000 (NanoDrop, Wilmington, DE, USA). The RNA integrity was assessed by Bioanalyzer 2100 (Agilent, CA, USA) with RIN number $>$7.0, and confirmed with denaturing agarose gel using electrophoresis. RNA sequencing analysis was performed following RNA extraction (Sequencing instrument: Illumina Novaseq 6000). The mRNA library was sequenced to a depth of 4G, with a read length of 150 bp using double-ended sequencing. Analyses were conducted on all the expression data samples derived from the self-tested PE dataset. Our internally generated dataset included transcriptional profiles from five preeclampsia cases, along with six matched control samples serving as the reference cohort. Detailed sample information is presented in Table 1. Following this, the internally compiled PE dataset was processed using the limma R package (version 3.52.0; R Foundation for Statistical Computing, Vienna, Austria) for standardization, including probe annotation and normalization to prepare for downstream analysis [8]. We generated side-by-side visualizations of the expression matrix across the batch-effect removal process, followed by principal component analysis to determine the effectiveness of the correction [9]. Principal component analysis (PCA) is a technique used for dimension reduction that transforms high-dimensional datasets into lower-dimensional representations. This process allows for effective visualization in two- or three-dimensional plots. The quality of sequencing data was rigorously controlled and evaluated. The integrity of RNA samples was

Table 1. Data set information list.

	PE-dataset
Species	Homo sapiens
Samples in the PE group	5
Samples in the Control group	6

PE, Preeclampsia.

detected using Agilent 2100 Bioanalyzer, with the RIN values all ≥7.0. The quality of data before and after sequencing is assessed based on a Q30 value of ≥90%. The original sequencing data were subjected to the removal of low-quality sequences and junction sequences by Trimmomatic, and then quality assessment was conducted using FastQC. To minimize the potential batch effect among samplesc. All processing steps follow standardized procedures to ensure data quality and the reliability of analytical results.

Genes Associated With Circadian Rhythm in the Self-Assessment PE Dataset

By systematically searching the published literature on PubMed with the keyword "Circadian Rhythm", the genetic information related to circadian rhythm was summarized and sorted out. After combining different literature sources and removing duplicate entries, 254 circadian rhythm-related genes (CRRGs) were finally obtained for subsequent analysis [10]. Based on the classification of samples within the self-assessment dataset PE, we categorized the subjects into the control and PE groups. Differential expression analysis was performed using limma in R, with thresholds set at $\log_2$FC >1 and p value < 0.05, and genes were classified as up- and down-regulated based on the direction of the $\log_2$FC. The findings were graphically summarized in a ggplot2-generated volcano plot.

Intersection of significant DEGs ($|\log_2 FC| > 1$, p value < 0.05) with circadian rhythm-related differentially expressed genes (CRRDEGs), which were then displayed in Venn and heatmap (heatmap R package). We classified the samples from the self-assessment PE dataset into two distinct groups: control and PE. To explore the expression differences of CRRDEGs between the two groups, we generated comparative charts reflecting the expression levels of these genes. ROC curves [11], also known as subject operating characteristic curves, were constructed as a valuable analytical tool for model evaluation and optimal threshold determination. The ROC curve provides an extensive metric by demonstrating the connection between sensitivity and specificity through a visual representation of continuous variables. We evaluated the diagnostic potential of CRRDEGs for PE by generating ROC curves and calculating corresponding AUC values via the pROC package. Diagnostic accuracy was classified based on AUC ranges as low (0.5–0.7), moderate (0.7–0.9), and high (>0.9).

Gene Set Enrichment Analysis (GSEA)

GSEA [12] enables functional interpretation of phenotype-associated gene rankings. Here, we first ordered genes in our PE dataset by $\log_2$FC, then performed GSEA using the clusterProfiler R package. The parameters for GSEA were set as follows: a seed value of 2020 with 1000 permutations. Each analyzed gene set contained a minimum of 10 genes and a maximum of 500 genes. For this analysis, we utilized the gene set "c2.cp.all.v2022.1.Hs.symbols.gmt", which encompasses all canonical pathways and consists of 3050 entries sourced from the Molecular Signatures Database (version 3.0) [13]. The statistical significance of the enrichment results was determined based on the FDR (q value) corrected by multiple tests. Pathways with FDR (q value) <0.05 were considered significantly enriched.

GO Enrichment Analysis

GO enrichment analysis [14] is a widely employed strategy for functional enrichment studies involving large-scale datasets of biological processes (BPs), cellular components (CCs), and molecular functions (MFs). In this study, for the differentially expressed genes related to circadian rhythms obtained through screening, Gene Ontology enrichment analysis was further performed to explain their potential biological functional characteristics. The significance of the enrichment items was evaluated based on the FDR (q value) corrected by the Benjamini-Hochberg method. An FDR <0.05 was considered indicative of statistically significant enrichment [15].

PPI Network

The PPI network is a complex framework composed of protein interactions that influences a range of BPs, including signal transduction, gene expression, metabolism, and the cell cycle. By analyzing these interactions in biological systems, we can understand the functions of these proteins and their complex relationships, along with their responses to specific physiological signals (such as in disease states).

The GeneMANIA [16] database (http://genemania.org) serves as a valuable online resource for analyzing gene functions within input gene lists and for predicting and prioritizing gene interactions. In this investigation, we utilized the GeneMANIA database to construct PPI networks based on CRRDEGs.

Proteins are vital for life, and comprehending their structures may improve our knowledge of their alignment functions. The AlphaFold website (https://www.alphafold.ebi.ac.uk/) [17] introduces an innovative computational approach to predict protein structures with atomic-level accuracy, even in the absence of homologous templates. This method has successfully predicted the structures of approximately 98.5% of known human proteins, with comparable success with other biological proteins. In our study, we

employed the Alphafold2 platform to forecast the protein structures of CRRDEGs within the PPI network and subsequently presented our findings.

Construct mRNA-miRNA, mRNA-TF and mRNA-Drug Interaction Networks

MicroRNAs (miRNAs) regulate the development and evolution of organisms by regulating their target genes, which may be controlled by multiple miRNAs. We retrieved and identified miRNAs related to CRRDEGs from the miRDB [18] database and explored their relationships with CRRDEGs. We subsequently visualized the mRNA-miRNA regulatory network using Cytoscape software(version 3.10.1; Cytoscape Consortium, San Diego, CA, USA).

TFs regulate gene expression at the post-transcriptional level by interacting with CRRDEGs. We studied the relationship between TFs and CRRDEGs using data from the ChIPBase database [19]. After the screening process, we visualized the mRNA-TF regulatory network.

Finally, the direct and indirect drug targets of the CRRDEGs were forecasted using the drug-gene interaction database (DGIdb) [20] (https://www.dgidb.org). The relationship between CRRDEGs and drugs was investigated, and the mRNA-drug regulatory network was visualized to complete the network construction.

Immune Infiltration Analysis

ssGSEA [21] evaluates the counterparts of by various immune cell types. Immune cell subtypes were identified and their infiltration levels quantified via ssGSEA enrichment. A significance-filtered matrix (p value < 0.05) was generated and visualized: ggplot2 highlighted inter-group differences, and heatmap illustrated immune–immune and immune–CRRDEG correlations.

The CIBERSORT [22] algorithm, applied with the LM22 signature, deconvolved immune cell abundances from expression data, yielding a filtered infiltration matrix. Inter-group differences were shown in ggplot2 proportion plots, and heatmaps presented LM22 immune cell correlations as well as their associations with CRRDEGs.

Statistical Analysis

All data analyses in this study were conducted in R software (version 4.2.2; R Foundation for Statistical Computing, Vienna, Austria). For the volcano plot of differential expression analysis, we use the linear model framework of the limma package. This method, which employs empirical Bayesian contraction of gene expression variance, is particularly suitable for the small-sample datasets and enables robust identification of differentially expressed genes across the entire genome. For the group comparisons (such as five key circadian rhythm-related differentially expressed genes, CRRDEGs), differences in their expression levels between the two groups were conducted using the Wilcoxon rank sum test (Mann-Whitney U test). The continuous results are expressed as mean $\pm$ standard deviation. For intergroup comparisons of three or more groups, the Kruskal-Wallis test was used. Categorical variables were compared using the chi-square test or Fisher's exact test. Correlation analysis was conducted using Spearman's rank correlation. Unless otherwise specified, a p value < 0.05 is considered statistically significant.

Results

The overall analysis process of this study is shown in Fig. 1.

The overall analysis process of this study included data collection and standardization, differential expression analysis, screening of circadian rhythmic-related genes, functional enrichment analysis and network construction. By integrating methods such as GSEA, GO, PPI and immune infiltration analysis, the potential mechanism of circadian rhythm-related genes in preeclampsia was systematically clarified.

Analysis of Circadian Rhythm-Related Differential Expression in the Self-Tested Dataset PE-Dataset

The self-tested PE dataset was first standardized using the limma, and comprised 11 samples, including 5 PE and 6 control samples. We demonstrated the results by drawing pre- and post-standardization group comparison (Fig. 2A,B) and PCA plots (Fig. 2C,D). As shown in Fig. 2A–D, standardization largely eliminated batch effects among samples, resulting in a comparable level of expression across the dataset.

Subsequently, the self-sequenced preeclampsia dataset was divided into a control group and a PE group. After performing data standardization and batch effect correction, differential expression analysis was conducted between the two groups using the limma R package to identify differentially expressed genes. Difference analysis was conducted using the R package limma, and the screening criteria were: $|\log_2 FC| > 1$ and p value < 0.05. The results were as follows: The PE dataset contained 373 expression genes that met the standards of $|\log_2 FC| > 1$ and p value < 0.05. Under this threshold, a total of 210 up-regulated expression genes ($|\log_2 FC| > 1$ and p value < 0.05) and 163 down-regulated expression genes ($|\log_2 FC| < -1$ and p value < 0.05) were detected. A volcano plot was constructed based on the results of this dataset (Fig. 3A).

To identify CRRDEGs associated with the PE dataset, we intersected DEGs and CRRGs that satisfied the thresholds of $|\log_2 FC| > 1$ and p value < 0.05, and visualized the results using a Venn diagram (Fig. 3B). Five CRRDEGs were identified: *MTTP*, *PROK1*, *UTS2*, *NKX2-1*, and *PRKAA2*. We examined the expression differences be-

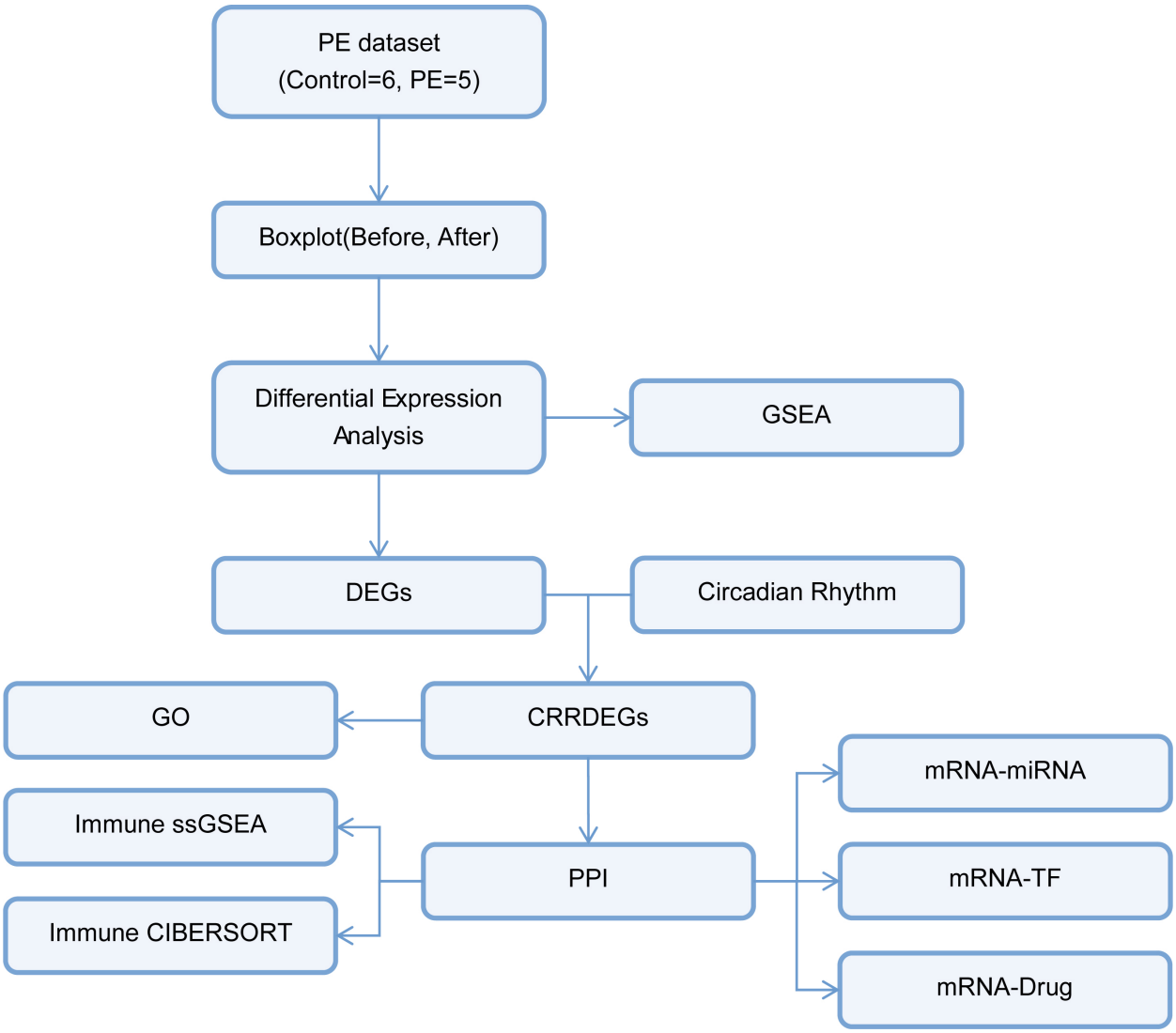

Fig. 1. The overall analysis process of this research. This figure presents the overall analysis process of the research, which consists of the main steps such as data preprocessing and standardization, screening of differentially expressed genes, identification of differentially expressed genes related to circadian rhythms, functional enrichment analysis, regulatory network construction, and immune infiltration analysis. PE, preeclampsia; DEGs, differentially expressed genes; CRRDEGs, circadian rhythm-related differentially expressed genes; PPI, protein-protein interaction; TF, transcription factors; GO, Gene Ontology; ssGSEA, single-sample gene set enrichment analysis; GSEA, gene set enrichment analysis. Flowcharts were drawn using Adobe Illustrator (version 2024; Adobe Inc., San Jose, CA, USA).

tween the PE and control groups in the self-tested PE dataset and visualized the results using a heat map (Fig. 3D).

To verify CRRDEGs, we drew a group comparison graph (Fig. 3C) for CRRDEGs based on the PE and control groups in the self-tested PE dataset. The findings indicated that two CRRDEGs (*PROK1* and *NKX2-1*) exhibited statistically significant differences across the groups in the self-tested PE dataset (p value < 0.05). To construct the ROC curve, two statistically significant CRRDEGs identified from the group comparison plots were selected and evaluated using the pROC package in R. The expression levels of CRRDEGs (*PROK1* and *NKX2-1*) demonstrated high accuracy for distinguishing the PE group, as shown by the ROC curve (Fig. 3E,F).

Gene Set Enrichment Analysis (GSEA)

To investigate the relationships between all gene expressions in the PE dataset and BPs, CCs, and MFs, GSEA was used, thereby identifying the influence of gene expression levels on PE in the PE dataset (Fig. 4A). The results are presented in Table 2. Significant enrichment in autophagy regulation (Fig. 4B), autoimmune thyroid diseases (Fig. 4C), translation (Fig. 4D), ribosomes (Fig. 4E), and other biologically relevant functions and signaling pathways was found in the PE dataset.

Functional enrichment analysis of circadian-associated DEGs highlighted their collective involvement in key pathways such as the regulation of autophagy,

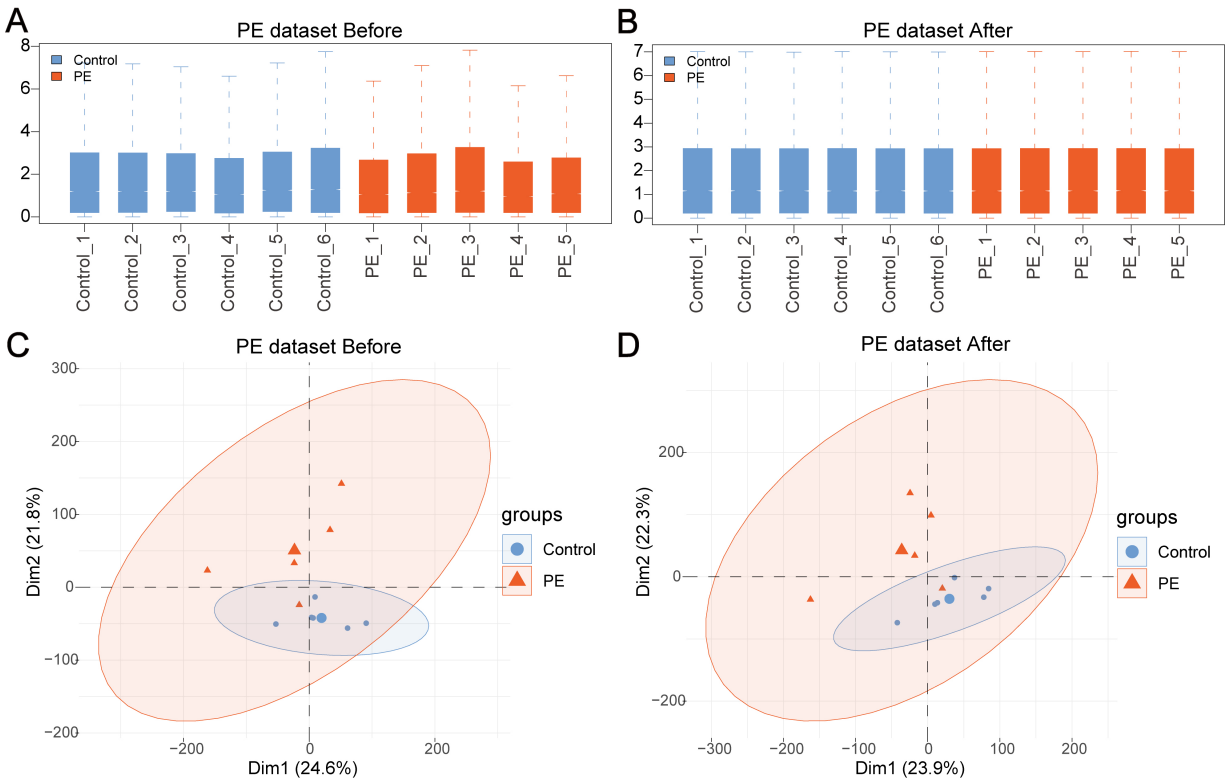

Fig. 2. DEGs of the self-tested PE dataset. Group comparison diagram of the self-tested PE dataset before (A) and after (B) standardized processing. PCA map of the PE dataset before (C) and after (D) standardized processing. In the group comparison chart, blue color represents the control group and red color represents the PE group. The vertical axes of Fig. 2A,B represent the expression levels of genes in the samples, showing the distribution of data before and after standardization. PE, preeclampsia; PCA, principal component analysis.

Table 2. GSEA results of the PE dataset.

Description	setSize	NES	*p*.adjust	q-values
KEGG_RIBOSOME	45	–2.90501	1.51×10^{-8}	1.41×10^{-8}
REACTOME_TRANSLATION	191	–2.30895	1.51×10^{-8}	1.41×10^{-8}
KEGG_AUTOIMMUNE_THYROID_DISEASE	31	1.910559	0.02025	0.018858
KEGG_REGULATION_OF_AUTOPHAGY	24	1.934225	0.030335	0.028249
WP_THYROXINE_THYROID_HORMONE_PRODUCTION	21	2.075458	0.003097	0.002884
REACTOME_METABOLISM_OF_AMINE_DERIVED_HORMONES	15	2.187275	0.000374	0.000348
WP_CYTOPLASMIC_RIBOSOMAL_PROTEINS	43	–2.83621	1.51×10^{-8}	1.41×10^{-8}
REACTOME_NONSENSE_MEDIATED_DECAY_NMD	63	–2.78251	1.51×10^{-8}	1.41×10^{-8}
REACTOME_EUKARYOTIC_TRANSLATION_INITIATION	67	–2.74218	1.51×10^{-8}	1.41×10^{-8}
REACTOME_SELENOAMINO_ACID_METABOLISM	68	–2.5598	1.51×10^{-8}	1.41×10^{-8}
REACTOME_INFLUENZA_INFECTION	95	–2.5504	1.51×10^{-8}	1.41×10^{-8}
REACTOME_REGULATION_OF_EXPRESSION_OF_SLITS_AND_ROBOS	106	–2.51889	1.51×10^{-8}	1.41×10^{-8}
REACTOME_CELLULAR_RESPONSE_TO_STARVATION	95	–2.42259	2.02×10^{-8}	1.88×10^{-8}
NABA_PROTEOGLYCANS	31	–2.34678	3×10^{-5}	2.79×10^{-5}
KEGG_COMPLEMENT_AND_COAGULATION_CASCADES	46	–2.33124	1.28×10^{-5}	1.19×10^{-5}

GSEA, gene set enrichment analysis.

immune-disease networks, protein translation machinery, and ribosome activity. These enriched pathways suggested that in preeclampsia samples, significant disorders may occur in cellular metabolism and immune response processes.

GO Enrichment Analysis

To further explore the potential connection between circadian rhythm-related differentially expressed genes and the immune microenvironment, this study analyzed the correlation between the expression level of CRRDEGs and

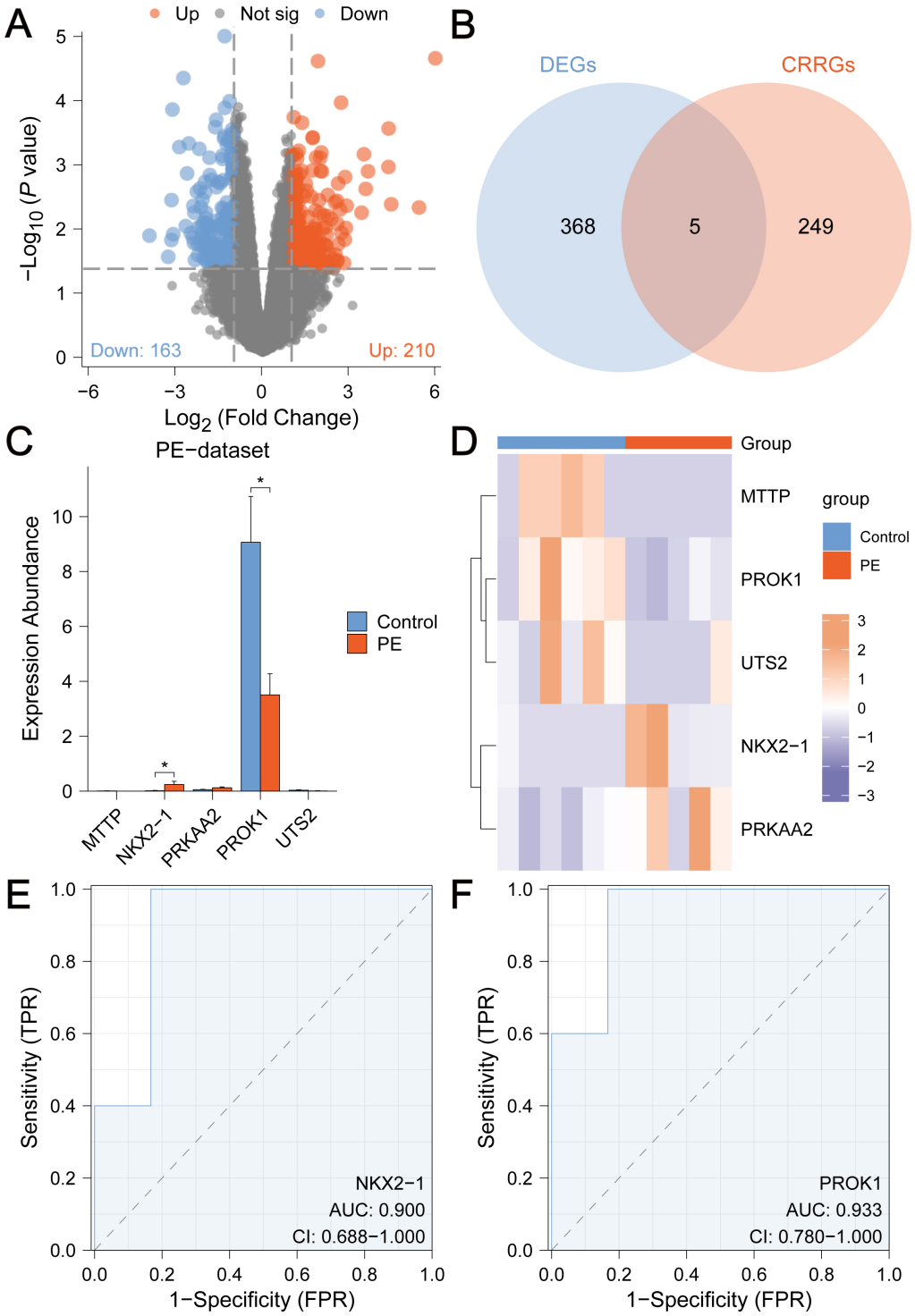

Fig. 3. Differential expression analysis of the self-tested PE dataset. (A) Differential gene analysis volcano maps of PE and control samples from the self-tested PE dataset. (B) Venn diagram of DEGs and CRRGs in the self-tested PE dataset. (C) CRRDEG group comparison diagram of the PE and control groups in the self-tested PE dataset. (D) CRRDEG heat maps in different groupings of the self-tested PE dataset (groupings: PE, Control). (E,F) CRRDEG (*NKX2-1* (E) and *PROK1* (F)) ROC curve in the self-tested PE dataset. PE, preeclampsia; CRRGs, circadian rhythm-related genes; CRRDEG, circadian rhythm-related differentially expressed gene; ROC, receiver operating characteristic curve; AUC, area under the curve. The closer the AUC is to 1, the better the diagnostic performance. AUC has a high accuracy above 0.9. In the group comparison chart and heat map, blue color represents the control group and red color represents the PE group. The color change from purple to orange in the heat map indicates low to high expression. * indicates p value $<$ 0.05.

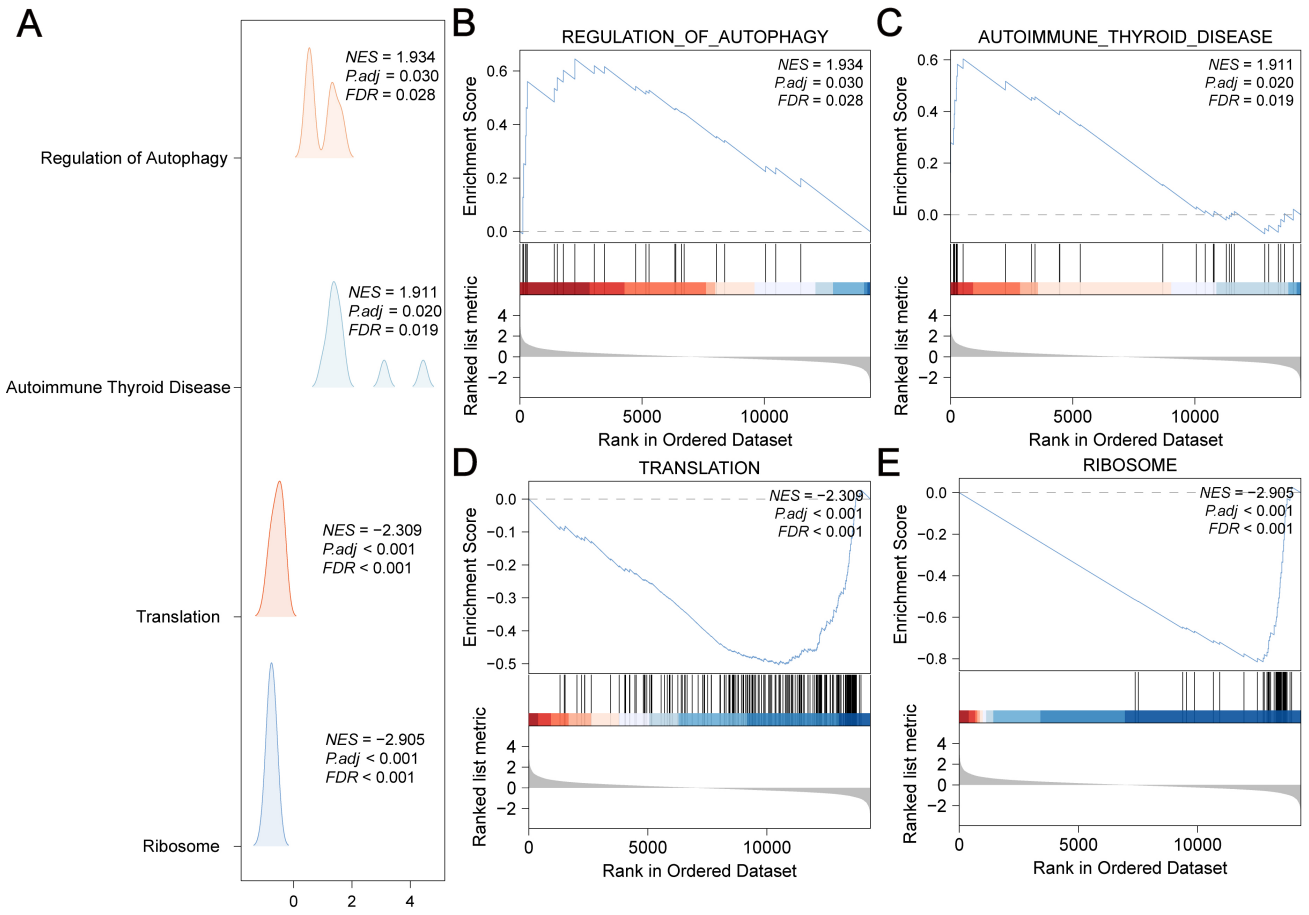

Fig. 4. GSEA of the self-tested PE dataset. (A) Four biological function mountain maps of GSEA of the self-tested PE dataset. (B–E) GSEA showing that all genes of the self-tested PE dataset are significantly enriched in REGULATION_OF_AUTOPHAGY (B), AUTOIMMUNE_THYROID_DISEASE (C), TRANSLATION (D), and RIBOSOMES (E). PE, preeclampsia; GSEA, gene set enrichment analysis. The screening criteria were FDR (q value) <0.05, and the correction method of FDR (q value) was Benjamini-Hochberg (BH).

the abundance of immune cell infiltration. The results showed that the changes in different gene expression were significantly correlated with the infiltration levels of specific immune cell types, suggesting that circadian rhythm-related genes may be involved in the immune regulatory process underlying preeclampsia. In the reported set of circadian rhythm-related genes, this study identified five genes (*MTTP*, *PROK1*, *UTS2*, *NKX2-1* and *PRKAA2*) that showed significant differential expression in preeclampsia samples. The differential expression of these genes suggested that circadian rhythm disorders may be involved in the occurrence and development of preeclampsia, providing clues for further research on its underlying mechanism. The GO enrichment analysis revealed that the differentially expressed genes were primarily involved in biological processes such as circadian rhythm regulation, response to calcium ions, and lipid homeostasis, indicating their potential roles in the physiological pathways related to preeclampsia. The results of the GO enrichment analysis are presented in a histogram format (Fig. 5A).

According to the findings of the GO enrichment analysis, a network illustration was developed for BPs and MFs (Fig. 5B,C). The line represents the associated molecules along with comments for each entry, and a larger node indicates that the entry contains more molecules.

The results of GO enrichment analysis showed that CRRDEGs were mainly involved in biological processes such as circadian rhythm regulation, calcium ion response and lipid homeostasis, and were significantly enriched in molecular functions such as receptor-ligand interaction and signal receptor activation. These functional items were closely related to the core pathological processes of preeclampsia, such as abnormal vascular tension, calcium signal imbalance and lipid metabolism disorders. The results suggested that genes related to circadian rhythms may affect placental vascular function and energy homeostasis by regulating calcium signaling pathways and lipid metabolism, providing new clues for clarifying the molecular mechanism of preeclampsia (Table 3).

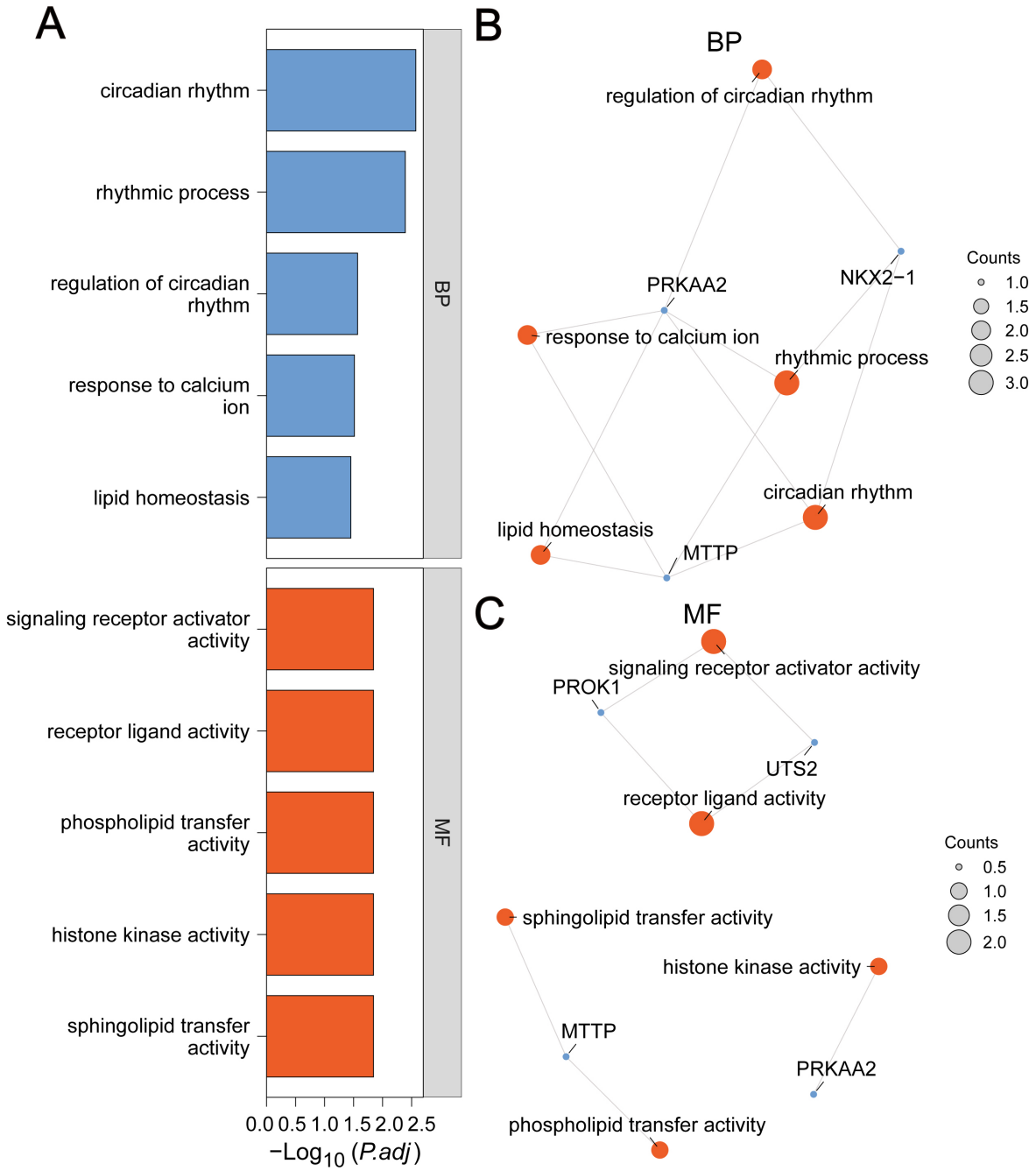

Fig. 5. GO enrichment analysis of CRRDEGs. (A) The results of GO enrichment analysis of 5 CRRDEGs are shown in the histogram: BPs and MFs. The horizontal coordinates are the GO terms. (B,C) The results of the GO enrichment analysis. CRRDEGs shown in the network diagram: BPs (B) and MFs (C). Red nodes represent entries, blue nodes represent molecules, and lines represent the relationships between entries and molecules. The screening criterion for GO enrichment analysis is an FDR (q value) <0.05. GO, Gene Ontology; BP, biological process; MF, molecular function.

PPI, mRNA-miRNA, mRNA-TF, and mRNA-Drug Networks

GeneMANIA-based (http://genemania.org) analysis prioritized CRRDEG interactions, demonstrating their connectivity via physical, co-expressive, predictive, co-localizational, genetic, and pathway-based associations (Fig. 6A). Structural predictions for corresponding proteins were acquired from the AlphaFold resource (https://www.alphafold.ebi.ac.uk/)—encompassing ~350,000 models spanning multiple species—and illustrated accordingly (Fig. 6B–F).

Initially, the miRNA regulatory network for CRRDEGs was constructed using the miRDB database and visualized with Cytoscape (Fig. 7A). Among them, 4 CR-

Table 3. GO enrichment analysis results.

Ontology	ID	Description	GeneRatio	BgRatio	*p*-value	*p*.adjust	q-value
BP	GO:0007623	circadian rhythm	3/5	205/18,800	1.26×10^{-5}	0.002678	0.001085
BP	GO:0048511	rhythmic process	3/5	297/18,800	3.81×10^{-5}	0.00406	0.001645
BP	GO:0042752	regulation of circadian rhythm	2/5	117/18,800	0.000379	0.026933	0.010914
BP	GO:0051592	response to calcium ion	2/5	144/18,800	0.000574	0.03056	0.012384
BP	GO:0055088	lipid homeostasis	2/5	173/18,800	0.000827	0.035219	0.014272
MF	GO:0120016	sphingolipid transfer activity	1/5	10/18,410	0.002713	0.014351	0.003941
MF	GO:0035173	histone kinase activity	1/5	16/18,410	0.004338	0.014351	0.003941
MF	GO:0120014	phospholipid transfer activity	1/5	24/18,410	0.006502	0.014351	0.003941
MF	GO:0048018	receptor ligand activity	2/5	489/18,410	0.006676	0.014351	0.003941
MF	GO:0030546	signaling receptor activator activity	2/5	496/18,410	0.006863	0.014351	0.003941

GO, Gene Ontology; BP, biological process; MF, molecular function.

RDEGs and 83 mismatches were included. For more details, please refer to Table 4.

Subsequently, we built and visualized the mRNA-TF regulatory network pertaining to CRRDEGs from the ChIPBase database (Fig. 7B). Three CRRDEGs and 26 TFs were included in the analysis. For more details, please refer to Table 5.

Ultimately, we identified potential drugs and molecular compounds associated with the CRRDEGs utilizing the DGIdb database. The first mRNA-drug regulatory network was constructed, which was then visualized using Cytoscape software (Fig. 7C). This network encompassed 2 CRRDEGs and 13 corresponding drugs or molecular compounds. A comprehensive summary of these findings is provided in Table 6.

The PPI network results indicated that there is a close physical interaction and co-expression relationship among CRRDEGs, suggesting that these genes exhibit a synergistic effect in signal transduction and metabolic regulation. The mrNA-mirNA and mrNA-TF regulatory networks revealed that these genes are influenced by multi-level transcriptional and post-transcriptional regulatory mechanisms. Candidate compounds identified in the drug-gene interaction network (such as statins, metformin) may exert their effects by regulating lipid metabolism and energy pathways. The overall network analysis results suggested that CRRDEGs are at the core of metabolism, inflammation and vascular function regulation, providing a theoretical basis for exploring targeted intervention for preeclampsia.

Self-Tested PE Dataset Immune Infiltration Analysis

ssGSEA-based infiltration analysis of the PE dataset revealed four immune cell types with significant intergroup differences: CD56 bright killer cells, central memory $CD8^+$ T cells, gamma-delta T cells, and monocytes (p value < 0.05; Fig. 8A), and their abundances correlated positively (Fig. 8B). The results of the correlation bubble chart showed that there was a significant positive correlation (r = 0.866) between CRRDEGs (*PROK1*) and immune cells (Central memory $CD8^+$ T cells). There was a significant negative correlation (r = –0.713) between CRRDEGs (*NKX2-1*) and immune cells (Central memory $CD8^+$ T cells). This result suggested that the expression levels of some circadian rhythm-related genes are closely related to the infiltration of specific immune cell subsets, reflecting that circadian rhythm genes may be involved in the occurrence and development of preeclampsia by regulating the immune environment.

CIBERSORT deconvolution of 22 immune subsets identified 19 present in the PE cohort (Fig. 8D), whose inter-correlations were predominantly negative (Fig. 8E). A concluding heatmap integrated CRRDEG expression with immune infiltration data (Fig. 8F), highlighting a positive *UTS2*–resting dendritic cell link and a negative *UTS2*–monocyte association.

The results of immune infiltration analysis showed significant differences in the abundance of multiple immune cell subsets between the PE group and the control group, especially $CD8^+$ T cells, Natural killer (NK) cells and monocytes. Some CRRDEGs (such as *PROK1*, *NKX2-1*, *UTS2*) were significantly correlated with specific immune cell types, suggesting that circadian rhythm genes may be involved in the pathological process of preeclampsia by regulating the immune microenvironment. These results revealed the potential link between circadian rhythm imbalance and immune dysfunction, providing new molecular evidence for further clarifying the immunological mechanism of preeclampsia (Fig. 8C).

Discussion

PE is a multifaceted multisystem disease that affects approximately 2–8% of pregnant women worldwide and is a major determinant of maternal and neonatal mortality [23]. It is characterized by the emergence of hypertension and proteinuria after the 20th week of pregnancy, potentially resulting in serious complications such as eclampsia, HELLP syndrome, and long-term cardiovascular risk in both mothers and their children [24]. The pathophysiology of PE remains incompletely understood; however,

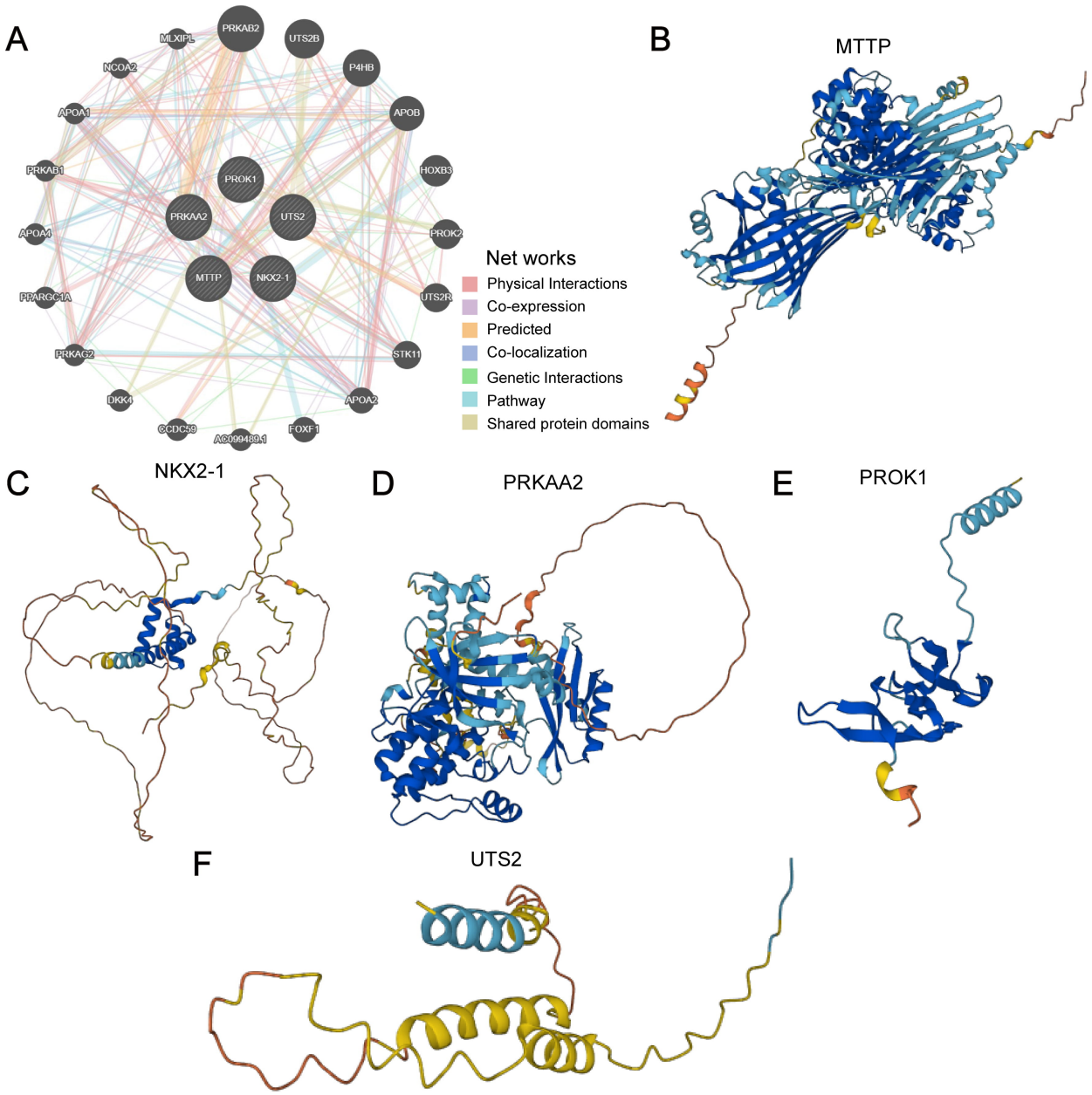

Fig. 6. Construction of the PPI interaction network. (A) CRRDEG GeneMANIA database analysis results. (B–F) Protein structure of CRRDEGs (MTTP (B), NKX2-1 (C), PRKAA2 (D), PROK1 (E), and UTS2 (F)). PPI, protein-protein interaction.

it is thought to be associated with abnormal placentation, immune dysregulation, endothelial dysfunction, and oxidative stress [25]. Considering the substantial health impact of PE, there is an urgent need to identify improved diagnostic markers and therapeutic targets to enhance disease management.

Recent studies have emphasized the possible involvement of CRRGs in the development of various diseases, including PE [26]. Circadian rhythms regulate physiological processes such as blood pressure and immune function that are disrupted in PE patients [27]. By profiling circadian rhythm gene expression alterations in PE, we pursued new mechanistic insights into this disorder.

PROK1, a secreted protein involved in angiogenesis and inflammation, is upregulated during various pregnancy-related complications [28]. Our study found that its presence in PE patients demonstrates high diagnostic accuracy (AUC $\geq$0.9), consistent with other studies, further supporting *PROK1* as a potential biomarker for the early detection of PE. It plays a prominent role in abnormal placentation and endothelial dysfunction [29]. Understanding how its expression is regulated by circadian rhythms could provide valuable insights into new intervention strategies. The key role of *MTTP* in lipid metabolism has also attracted our attention. The observed dysregulation of lipids in PE patients is closely related to the expression of *MTTP*, which

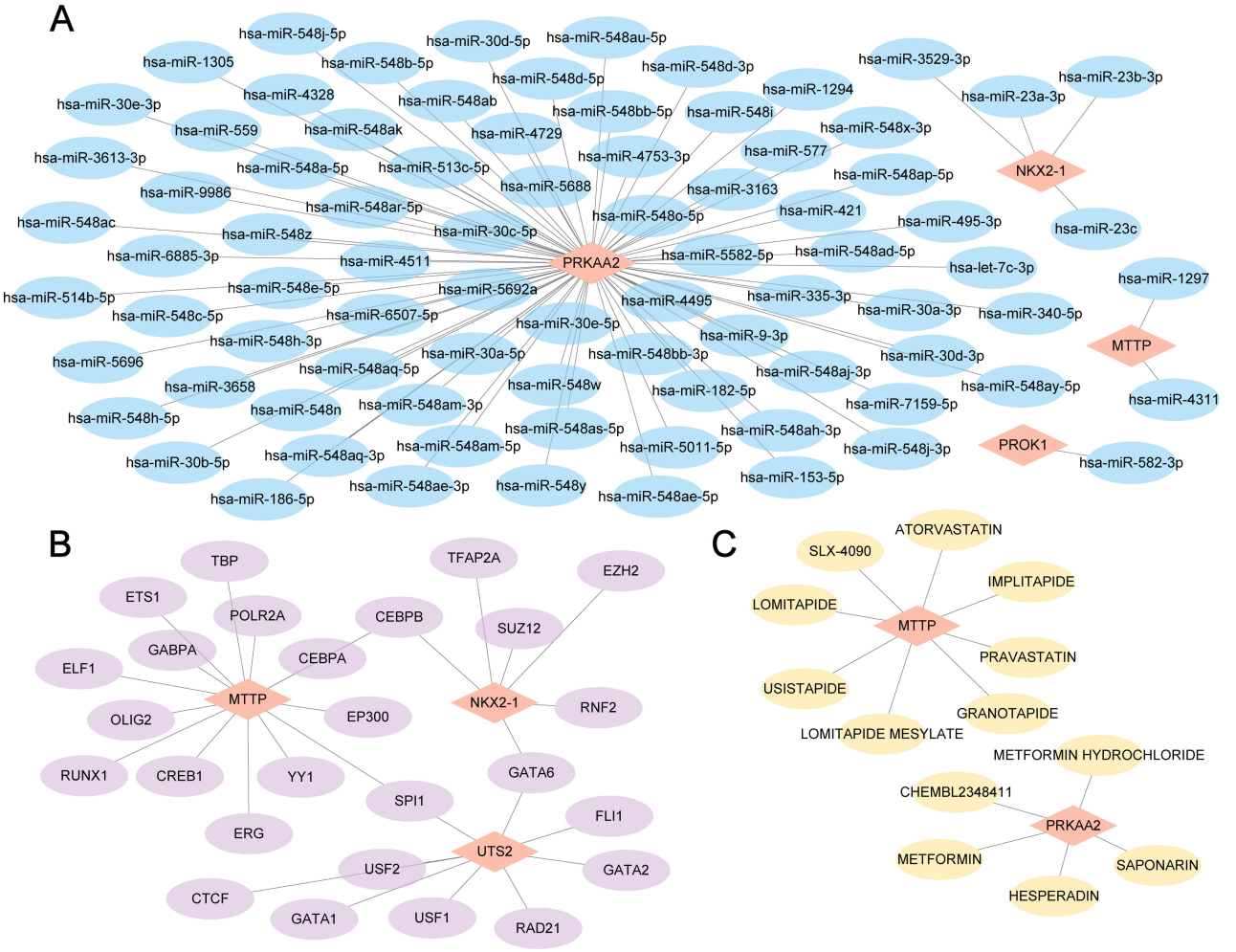

Fig. 7. mRNA-miRNA, mRNA-TF, and mRNA-drug interaction networks. (A) mRNA-miRNA regulatory network of CRRDEGs. (B) mRNA-TF regulatory network of CRRDEGs. (C) mRNA-drug regulatory network of CRRDEGs. Red color represents mRNA, purple color represents TFs, blue color represents miRNA, and yellow color represents drugs. TFs, transcription factors; CRRDEGs, circadian rhythm-related differentially expressed genes.

is consistent with prior research and emphasizes the significance of disturbances in lipid metabolism in the pathophysiology of PE [30]. Our results reveal that *MTTP*, as a CRRDEG, may be involved in the disruption of metabolic processes influenced by circadian rhythms, providing new directions for future research. *UTS2*, as a vasoactive peptide, drew our attention due to its strong vasoconstrictive effects [31]. Although existing studies have explored its role in cardiovascular diseases, its role in PE remains unclear. Our research suggests its potential involvement in blood pressure regulation, which may encourage further exploration of the pathological mechanisms of *UTS2* in PE.

In this study, PROK1 and NKX2-1, identified as core circadian rhythm-related genes in preeclampsia, both yielded AUC values $\geq$0.9 on ROC curves, indicating their excellent diagnostic accuracy for the disease. This finding is supported by a certain degree of theoretical rationale: PROK1 and NKX2-1 are key regulators of circadian rhythms, and GO enrichment analysis confirmed their involvement in circadian regulation, calcium ion response, and lipid homeostasis—biological processes whose disruption is central to the vascular endothelial injury and placental dysfunction characteristic of preeclampsia. Regarding the reliability of our results, the raw data underwent rigorous standardization and batch-effect correction, with PCA analysis confirming acceptable sample quality. Differential gene expression was filtered using stringent thresholds of $|\log_2 FC| > 1$ and $p < 0.05$, and AUC values were calculated following standardized protocols using the pROC package, ensuring methodological robustness and reproducible results.

Nevertheless, potential sources of bias should be acknowledged. First, the limited sample size may contribute to result bias. Second, clinical confounding factors such as gestational age, maternal age, and disease severity were not included in the adjustment. Additionally, the specific tissue type of the samples was not specified, and tissue specificity may affect the clinical applicability of these diagnos-

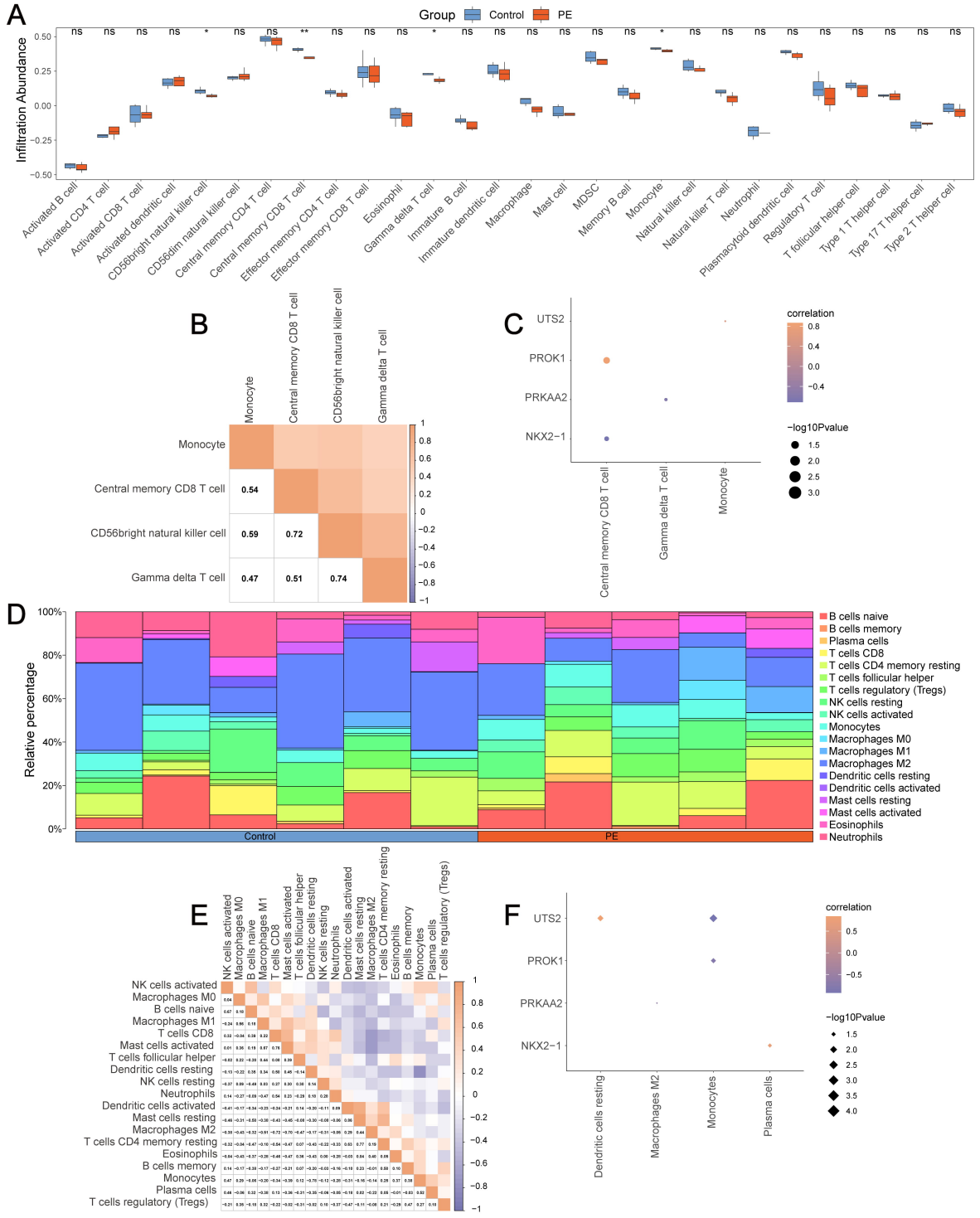

Fig. 8. Immune infiltration analysis of the self-tested PE dataset. (A) Group comparison of ssGSEA immune infiltration results of the self-tested PE dataset. (B) Correlation analysis results of the immune cell infiltration abundance of the self-tested PE dataset. (C) Correlation point plot of immune cells and CRRDEGs in the self-tested PE dataset. (D) Histogram of CIBERSORT immune infiltration analysis results of the self-tested PE dataset. (E) Correlation analysis results of the immune cell infiltration abundance of the self-tested PE dataset. (F) Correlation point plot of immune cells and CRRDEGs in the self-tested PE dataset. ns is equal to p value ≥ 0.05, which has no statistical significance. * indicates p value < 0.05; ** indicates p value < 0.01. The value in the lower left corner of the correlation point plot is the correlation coefficient (R value). The figure in the lower left corner of the correlation heat map represents the correlation coefficient (R). The absolute value of the correlation coefficient (R) below 0.3 indicates weak or no correlation, R between 0.3 and 0.5 indicates a weak correlation, R between 0.5 and 0.8 indicates moderate correlation, and R above 0.8 indicates a strong correlation. PE, preeclampsia; ssGSEA, single-sample gene set enrichment analysis.

Table 4. mRNA-miRNA interaction network nodes.

miRNA		mRNA	miRNA		mRNA
hsa-miR-3529-3p	-	*NKX2-1*	hsa-miR-548d-5p	-	*PRKAA2*
hsa-miR-30d-3p	-	*PRKAA2*	hsa-miR-548h-5p	-	*PRKAA2*
hsa-miR-5582-5p	-	*PRKAA2*	hsa-miR-548a-5p	-	*PRKAA2*
hsa-miR-30a-3p	-	*PRKAA2*	hsa-miR-548i	-	*PRKAA2*
hsa-miR-9-3p	-	*PRKAA2*	hsa-miR-548as-5p	-	*PRKAA2*
hsa-miR-30e-3p	-	*PRKAA2*	hsa-miR-548w	-	*PRKAA2*
hsa-miR-4328	-	*PRKAA2*	hsa-let-7c-3p	-	*PRKAA2*
hsa-miR-548ae-3p	-	*PRKAA2*	hsa-miR-548ab	-	*PRKAA2*
hsa-miR-548aq-3p	-	*PRKAA2*	hsa-miR-548ay-5p	-	*PRKAA2*
hsa-miR-548n	-	*PRKAA2*	hsa-miR-548o-5p	-	*PRKAA2*
hsa-miR-548ah-3p	-	*PRKAA2*	hsa-miR-548ap-5p	-	*PRKAA2*
hsa-miR-548j-3p	-	*PRKAA2*	hsa-miR-548ar-5p	-	*PRKAA2*
hsa-miR-548am-3p	-	*PRKAA2*	hsa-miR-548au-5p	-	*PRKAA2*
hsa-miR-548x-3p	-	*PRKAA2*	hsa-miR-548y	-	*PRKAA2*
hsa-miR-548aj-3p	-	*PRKAA2*	hsa-miR-548ae-5p	-	*PRKAA2*
hsa-miR-7159-5p	-	*PRKAA2*	hsa-miR-548am-5p	-	*PRKAA2*
hsa-miR-421	-	*PRKAA2*	hsa-miR-548aq-5p	-	*PRKAA2*
hsa-miR-5692a	-	*PRKAA2*	hsa-miR-548ak	-	*PRKAA2*
hsa-miR-1305	-	*PRKAA2*	hsa-miR-4753-3p	-	*PRKAA2*
hsa-miR-1294	-	*PRKAA2*	hsa-miR-548bb-5p	-	*PRKAA2*
hsa-miR-9986	-	*PRKAA2*	hsa-miR-23a-3p	-	*NKX2-1*
hsa-miR-186-5p	-	*PRKAA2*	hsa-miR-23b-3p	-	*NKX2-1*
hsa-miR-5011-5p	-	*PRKAA2*	hsa-miR-23c	-	*NKX2-1*
hsa-miR-577	-	*PRKAA2*	hsa-miR-30a-5p	-	*PRKAA2*
hsa-miR-153-5p	-	*PRKAA2*	hsa-miR-548h-3p	-	*PRKAA2*
hsa-miR-5688	-	*PRKAA2*	hsa-miR-548ac	-	*PRKAA2*
hsa-miR-5696	-	*PRKAA2*	hsa-miR-548d-3p	-	*PRKAA2*
hsa-miR-3658	-	*PRKAA2*	hsa-miR-182-5p	-	*PRKAA2*
hsa-miR-4729	-	*PRKAA2*	hsa-miR-30c-5p	-	*PRKAA2*
hsa-miR-6507-5p	-	*PRKAA2*	hsa-miR-30b-5p	-	*PRKAA2*
hsa-miR-4311	-	*MTTP*	hsa-miR-30d-5p	-	*PRKAA2*
hsa-miR-1297	-	*MTTP*	hsa-miR-548bb-3p	-	*PRKAA2*
hsa-miR-548j-5p	-	*PRKAA2*	hsa-miR-30e-5p	-	*PRKAA2*
hsa-miR-335-3p	-	*PRKAA2*	hsa-miR-548z	-	*PRKAA2*
hsa-miR-514b-5p	-	*PRKAA2*	hsa-miR-582-3p	-	*PROK1*
hsa-miR-559	-	*PRKAA2*	hsa-miR-3163	-	*PRKAA2*
hsa-miR-548c-5p	-	*PRKAA2*	hsa-miR-4511	-	*PRKAA2*
hsa-miR-495-3p	-	*PRKAA2*	hsa-miR-548e-5p	-	*PRKAA2*
hsa-miR-6885-3p	-	*PRKAA2*	hsa-miR-340-5p	-	*PRKAA2*
hsa-miR-513c-5p	-	*PRKAA2*	hsa-miR-3613-3p	-	*PRKAA2*
hsa-miR-548b-5p	-	*PRKAA2*	hsa-miR-4495	-	*PRKAA2*
hsa-miR-548ad-5p	-	*PRKAA2*			

"miRNA" and "mRNA" represent nodes and "-" represents edge.

Table 5. mRNA-TF interaction network nodes.

TF		mRNA	TF		mRNA
ERG	-	*MTTP*	*EZH2*	-	*NKX2-1*
GABPA	-	*MTTP*	*SUZ12*	-	*NKX2-1*
RUNX1	-	*MTTP*	*TBP*	-	*MTTP*
CTCF	-	*UTS2*	*USF1*	-	*UTS2*
SPI1	-	*MTTP*	*RNF2*	-	*NKX2-1*
CEBPB	-	*NKX2-1*	*ETS1*	-	*MTTP*
ELF1	-	*MTTP*	*FLI1*	-	*UTS2*
POLR2A	-	*MTTP*	*GATA1*	-	*UTS2*
RAD21	-	*UTS2*	*GATA6*	-	*UTS2*
GATA6	-	*NKX2-1*	*SPI1*	-	*UTS2*
EP300	-	*MTTP*	*USF2*	-	*UTS2*
YY1	-	*MTTP*	*TFAP2A*	-	*NKX2-1*
CEBPB	-	*MTTP*	*OLIG2*	-	*MTTP*
CREB1	-	*MTTP*	*CEBPA*	-	*MTTP*
GATA2	-	*UTS2*	*EZH2*	-	*NKX2-1*

"mRNA" and "TF" represent nodes; "-" represents an edge. TF, transcription factors.

tic markers. In future studies, we will expand the sample size, incorporate multi-center external validation, and develop combined diagnostic models integrating clinical indicators to further enhance the reliability and clinical translational value of our findings.

GSEA demonstrated notable enrichment in autophagy regulation, autoimmune thyroid disease, transcriptional activities, and ribosomal functions within the PE dataset. Autophagy is a cellular degradation mechanism essential for preserving cellular homeostasis and is associated with several pregnancy-related complications, including PE [32]. The association with autoimmune thyroid diseases suggests a potential autoimmune component in PE, which aligns with previous findings indicating that alterations in immune tolerance may contribute to its pathogenesis [33]. Transcriptional processes are fundamental to the regulation of gene expression, and their disruption can lead to aberrant expression patterns observed in PE. Moreover, ribosomes are essential for protein synthesis, and defects in ribosomal function have been linked to stress responses and cellular dysfunction [34].

GO enrichment analysis based on the identified CRRDEGs highlighted their involvement in BPs such as circadian rhythm regulation, calcium ion response, and lipid homeostasis. Circadian rhythms influence various physiological processes, including hormonal secretion and cardiovascular function, and disruptions in these rhythms may exacerbate conditions such as PE [35,36]. Calcium signaling plays a pivotal role in vascular smooth muscle function, and its dysregulation is associated with hypertension, a key feature of PE [37]. Alterations in lipid metabolism have also been reported in PE patients, suggesting that lipid homeostasis is critical for maintaining normal placental function [38].

The enriched pathways provide critical insights into the molecular mechanisms involved in PE progression. By elucidating these pathways, we obtained more comprehensive insights into the etiology of this multifaceted disorder, while simultaneously opening new avenues for the identification of novel therapeutic targets aimed at modulating these BPs. The enriched pathways provided crucial insights into the molecular mechanisms underlying the progression

Table 6. mRNA-drug interaction network nodes.

Drug		mRNA	Drug		mRNA
LOMITAPIDE MESYLATE	-	*MTTP*	ATORVASTATIN	-	*MTTP*
IMPLITAPIDE	-	*MTTP*	METFORMIN	-	*PRKAA2*
LOMITAPIDE	-	*MTTP*	METFORMIN HYDROCHLORIDE	-	*PRKAA2*
SLX-4090	-	*MTTP*	CHEMBL2348411	-	*PRKAA2*
PRAVASTATIN	-	*MTTP*	HESPERADIN	-	*PRKAA2*
GRANOTAPIDE	-	*MTTP*	SAPONARIN	-	*PRKAA2*
USISTAPIDE	-	*MTTP*			

"Drug" and "mRNA" represent nodes; "-" represents an edge.

of PE. A comprehensive understanding of these pathways not only clarifies the etiology of this intricate disorder but also facilitates the identification of novel therapeutic targets focused on modulating these BPs.

Our analysis of immune cell infiltration revealed discrepancies among four types of immune cells in the PE and control groups, with certain CRRDEGs demonstrating strong correlations with specific immune cell infiltrates. This indicates that the immune system may be crucial in the development of PE, with certain genes potentially influencing this process by affecting immune cell function [39]. For instance, Tregs, which maintain immunological tolerance, were altered in the present study. Treg dysregulation has been associated with adverse pregnancy outcomes, including PE [40]. Similarly, changes in natural killer cell populations, which are crucial for early placental development and maternal-fetal tolerance, may contribute to the abnormal placentation observed in PE [41].

Moreover, our findings align with previous studies indicating that an imbalance between pro-inflammatory and anti-inflammatory cytokines could lead to a systemic inflammatory state characteristic of PE [33]. The relationship between CRRDEGs and the levels of particular immune cells highlights a possible mechanistic connection between the dysregulation of circadian gene expression and immune responses in PE. Considering that circadian rhythms affect multiple facets of immune function [26], it is plausible that disruptions in these rhythms may exacerbate inflammatory processes or alter immunological tolerance during pregnancy.

Although this study provides important insights into the changes in CRRG expression and their potential biological roles and diagnostic value in PE, several limitations should be acknowledged. First, this study was based on a self-constructed small RNA-seq cohort and systematically analyzed the differentially expressed circadian rhythm-related genes between PE and control samples. It further proposes a combination of molecular markers with potential diagnostic value, providing a theoretical basis for early molecular classification and intervention of PE. However, due to the limited number of PE samples and data heterogeneity in public databases, the current results have not yet been externally validated in independent datasets. Moreover, the scoring system remains only a preliminary exploratory combination of markers, lacking multi-center validation, generalizability and clinical applicability. Future research will include multi-center cohorts and functional experiments to further enhance the robustness and scientific significance of the model. Second, the relatively small sample size limits the statistical power, affecting the generalizability of the conclusions. Third, due to the constraints of existing data, more detailed biological information about participants, such as genetic background, lifestyle factors, and environmental influences, could not be obtained, which may hinder a deeper understanding of the mechanisms of action of the biomarkers. Fourth, principal component analysis revealed that although the PE and the control groups showed a clearer separation trend in the overall expression profile after batch effect correction, there was still a certain degree of variability within the PE group. This intra-group heterogeneity may be related to the differences in the clinical severity, onset time and underlying pathological mechanisms of preeclampsia, and it may also reflect the natural variations in molecular characteristics among individuals. Finally, there is a lack of further validation using clinical samples and laboratory wet experiments, and the diagnostic and therapeutic value of the identified CRRDEGs has yet to be assessed in a clinical setting. To address these limitations, future research should expand the sample size, enrich the collection of biological and clinical information, and broaden the database search while incorporating experimental validation to enhance the scientific and practical value of the study's conclusions.

In summary, our study identified potential biomarkers for the diagnosis of PE and described the correlations between PE, CRRDEGs, and the immune system. These findings are crucial for understanding the molecular mechanisms of PE and suggest potential therapeutic targets that can regulate circadian rhythms and immune responses, ultimately improving pregnancy outcomes.

Conclusions

We conducted systematic profiling of circadian rhythm gene expression and function in PE using RNA-seq and bioinformatic analyses. Among five key circadian-

related DEGs identified (*MTTP*, *PROK1*, *UTS2*, *NKX2-1*, and *PRKAA2*), *PROK1* and *NKX2-1* displayed strong diagnostic performance (AUC $\geq$0.9), indicating biomarker utility. Functional enrichment highlighted their participation in circadian, metabolic, calcium, autophagic, and immune pathways, suggesting a multi-faceted regulatory network in disease development. Additionally, immune infiltration analysis showed significant associations between CRRDEG expression and shifts in specific immune cell subsets—including memory $CD8^+$ T cells, NK cells, and monocytes—implying that circadian disturbances may influence PE through immune modulation.

This research offers new insights into PE pathogenesis and identifies molecular foundations for improved diagnostic and therapeutic strategies. Circadian gene expression alterations emerge as a promising clinical target for prediction and management. Further validation in larger, diverse cohorts and mechanistic studies is needed to clarify the circadian-immune crosstalk in PE. Overall, our study systematically demonstrates a molecular association between circadian disruption and preeclampsia, laying a conceptual groundwork for circadian-based clinical applications.

Availability of Data and Materials

The data that support the findings of this study are available on request from the corresponding author. The data are not publicly available due to privacy or ethical restrictions.

Author Contributions

YQX conceived the study, collected the data, and drafted the manuscript. TXZ and XM conducted statistical analysis and participated in the drafting of the manuscript. JL and MJ analyzed, interpreted data and participated in drafting the paper manuscripts. XXJ and FQ designed the study and critically revised the manuscript for important intellectual content. All authors gave final approval of the version to be published. All authors have participated sufficiently in the work to take public responsibility for appropriate portions of the content and agreed to be accountable for all aspects of the work in ensuring that questions related to its accuracy or integrity.

Ethics Approval and Consent to Participate

Our study has been approved by the Medical Ethics Committee of Taizhou Hospital of Zhejiang Province and its affiliated institution, Taizhou Hospital of Zhejiang Province (Approval number is K20210733). In accordance with the ethical principles outlined in the Declaration of Helsinki, all participants provided informed consent prior to participating in the study. Participant anonymity and confidentiality are ensured, and participation is entirely voluntary.

Acknowledgment

Not applicable.

Funding

This study is supported by Medical Science and Technology Project of Zhejiang Province (2024KY526), Science and Technology Plan Project of Taizhou (21ywa09).

Conflict of Interest

The authors declare no conflict of interest.

References

[1] Magee LA, Nicolaides KH, von Dadelszen P. Preeclampsia. The New England Journal of Medicine. 2022; 386: 1817–1832. https://doi.org/10.1056/NEJMra2109523.

[2] Tlaye KG, Endalfer ML, Kassaw MW, Gebremedhin MM, Aynalem YA. Preeclampsia management modalities and perinatal death: a retrospective study in Woldia general hospital. BMC Pregnancy and Childbirth. 2020; 20: 205. https://doi.org/10.1186/s12884-020-02909-9.

[3] Steegers EAP, von Dadelszen P, Duvekot JJ, Pijnenborg R. Pre-eclampsia. Lancet (London, England). 2010; 376: 631–644. https://doi.org/10.1016/S0140-6736(10)60279-6.

[4] Lebailly B, Boitard C, Rogner UC. Circadian rhythm-related genes: implication in autoimmunity and type 1 diabetes. Diabetes, Obesity & Metabolism. 2015; 17: 134–138. https://doi.org/10.1111/dom.12525.

[5] Giebfried J, Lorentz A. Relationship between the Biological Clock and Inflammatory Bowel Disease. Clocks & Sleep. 2023; 5: 260–275. https://doi.org/10.3390/clockssleep5020021.

[6] Diallo AB, Coiffard B, Desbriere R, Katsogiannou M, Donato X, Bretelle F, *et al*. Disruption of the Expression of the Placental Clock and Melatonin Genes in Preeclampsia. International Journal of Molecular Sciences. 2023; 24: 2363. https://doi.org/10.3390/ijms24032363.

[7] Venegas C, Jara-Medina K, Cueto N, Cabello-Guzmán G, Lagunas C, Lillo L, *et al*. Melatonin modulates the gene expression of WEE1 kinase and clock genes: a crosstalk between the molecular clocks of the placenta? Frontiers in Endocrinology. 2025; 16: 1640635. https://doi.org/10.3389/fendo.2025.1640635.

[8] Baker BH, Sathyanarayana S, Szpiro AA, MacDonald JW, Paquette AG. RNAseqCovarImpute: a multiple imputation procedure that outperforms complete case and single imputation differential expression analysis. Genome Biology. 2024; 25: 236. https://doi.org/10.1186/s13059-024-03376-7.

[9] Ben Salem K, Ben Abdelaziz A. Principal Component Analysis (PCA). La Tunisie Medicale. 2021; 99: 383–389.

[10] Zhou R, Chen X, Liang J, Chen Q, Tian H, Yang C, *et al*. A circadian rhythm-related gene signature associated with tumor immunity, cisplatin efficacy, and prognosis in bladder cancer. Aging. 2021; 13: 25153–25179. https://doi.org/10.18632/aging.203733.

[11] Mandrekar JN. Receiver operating characteristic curve in diagnostic test assessment. Journal of Thoracic Oncology: Official Publication of the International Association for the Study of Lung Cancer. 2010; 5: 1315–1316. https://doi.org/10.1097/JTO.0b013e3181ec173d.

[12] Subramanian A, Tamayo P, Mootha VK, Mukherjee S, Ebert BL, Gillette MA, *et al*. Gene set enrichment analysis: a knowledge-based approach for interpreting genome-wide expression pro-

files. Proceedings of the National Academy of Sciences of the United States of America. 2005; 102: 15545–15550. https://doi.org/10.1073/pnas.0506580102.

[13] Liberzon A, Subramanian A, Pinchback R, Thorvaldsdóttir H, Tamayo P, Mesirov JP. Molecular signatures database (MSigDB) 3.0. Bioinformatics (Oxford, England). 2011; 27: 1739–1740. https://doi.org/10.1093/bioinformatics/btr260.

[14] Thomas PD, Ebert D, Muruganujan A, Mushayahama T, Albou LP, Mi H. PANTHER: Making genome-scale phylogenetics accessible to all. Protein Science: a Publication of the Protein Society. 2022; 31: 8–22. https://doi.org/10.1002/pro.4218.

[15] Yu G, Wang LG, Han Y, He QY. clusterProfiler: an R package for comparing biological themes among gene clusters. Omics: a Journal of Integrative Biology. 2012; 16: 284–287. https://doi.org/10.1089/omi.2011.0118.

[16] Franz M, Rodriguez H, Lopes C, Zuberi K, Montojo J, Bader GD, *et al*. GeneMANIA update 2018. Nucleic Acids Research. 2018; 46: W60–W64. https://doi.org/10.1093/nar/gky311.

[17] Varadi M, Anyango S, Deshpande M, Nair S, Natassia C, Yordanova G, *et al*. AlphaFold Protein Structure Database: massively expanding the structural coverage of protein-sequence space with high-accuracy models. Nucleic Acids Research. 2022; 50: D439–D444. https://doi.org/10.1093/nar/gkab1061.

[18] Chen Y, Wang X. miRDB: an online database for prediction of functional microRNA targets. Nucleic Acids Research. 2020; 48: D127–D131. https://doi.org/10.1093/nar/gkz757.

[19] Zhou KR, Liu S, Sun WJ, Zheng LL, Zhou H, Yang JH, *et al*. ChIPBase v2.0: decoding transcriptional regulatory networks of non-coding RNAs and protein-coding genes from ChIP-seq data. Nucleic Acids Research. 2017; 45: D43–D50. https://doi.org/10.1093/nar/gkw965.

[20] Cannon M, Stevenson J, Stahl K, Basu R, Coffman A, Kiwala S, *et al*. DGIdb 5.0: rebuilding the drug-gene interaction database for precision medicine and drug discovery platforms. Bioinformatics. 2024; 40: btae366. https://doi.org/10.1093/bioinformatics/btae366

[21] Xiao B, Liu L, Li A, Xiang C, Wang P, Li H, *et al*. Identification and Verification of Immune-Related Gene Prognostic Signature Based on ssGSEA for Osteosarcoma. Frontiers in Oncology. 2020; 10: 607622. https://doi.org/10.3389/fonc.2020.607622.

[22] Newman AM, Liu CL, Green MR, Gentles AJ, Feng W, Xu Y, *et al*. Robust enumeration of cell subsets from tissue expression profiles. Nature Methods. 2015; 12: 453–457. https://doi.org/10.1038/nmeth.3337.

[23] Mol BWJ, Roberts CT, Thangaratinam S, Magee LA, de Groot CJM, Hofmeyr GJ. Pre-eclampsia. Lancet (London, England). 2016; 387: 999–1011. https://doi.org/10.1016/S0140-6736(15)00070-7.

[24] Filipek A, Jurewicz E. Preeclampsia - a disease of pregnant women. Postepy Biochemii. 2018; 64: 232–229. https://doi.org/10.18388/pb.2018_146. (In Polish)

[25] Levine RJ, Maynard SE, Qian C, Lim KH, England LJ, Yu KF, *et al*. Circulating angiogenic factors and the risk of preeclampsia. The New England Journal of Medicine. 2004; 350: 672–683. https://doi.org/10.1056/NEJMoa031884.

[26] Tang J, Dong Q, Chen X. Identification of potential circadian rhythm-related hub genes and immune infiltration in preeclampsia through bioinformatics analysis. Hypertension in Pregnancy. 2025; 44: 2559734. https://doi.org/10.1080/10641955.2025.2559734.

[27] Hermida RC, Ayala DE, Mojón A, Fernández JR. Influence of circadian time of hypertension treatment on cardiovascular risk: results of the MAPEC study. Chronobiology International. 2010; 27: 1629–1651. https://doi.org/10.3109/07420528.2010.510230.

[28] Alfaidy N. Prokineticin1 and pregnancy. Annales D'endocrinologie. 2016; 77: 101–104. https://doi.org/10.1016/j.ando.2016.04.014.

[29] Sergent F, Vaiman D, Raia-Barjat T, Younes H, Marquette C, Desseux M, *et al*. Antagonisation of Prokineticin Receptor-2 Attenuates Preeclampsia Symptoms. Journal of Cellular and Molecular Medicine. 2025; 29: e70346. https://doi.org/10.1111/jcmm.70346.

[30] Poornima IG, Indaram M, Ross JD, Agarwala A, Wild RA. Hyperlipidemia and risk for preclampsia. Journal of Clinical Lipidology. 2022; 16: 253–260. https://doi.org/10.1016/j.jacl.2022.02.005.

[31] Ames RS, Sarau HM, Chambers JK, Willette RN, Aiyar NV, Romanic AM, *et al*. Human urotensin-II is a potent vasoconstrictor and agonist for the orphan receptor GPR14. Nature. 1999; 401: 282–286. https://doi.org/10.1038/45809.

[32] Jin J, Gao L, Zou X, Zhang Y, Zheng Z, Zhang X, *et al*. Gut Dysbiosis Promotes Preeclampsia by Regulating Macrophages and Trophoblasts. Circulation Research. 2022; 131: 492–506. https://doi.org/10.1161/CIRCRESAHA.122.320771.

[33] Islam MM, Takeyama N. Role of Neutrophil Extracellular Traps in Health and Disease Pathophysiology: Recent Insights and Advances. International Journal of Molecular Sciences. 2023; 24: 15805. https://doi.org/10.3390/ijms242115805.

[34] Gościńska K, Topf U. The evolving role of ribosomes in the regulation of protein synthesis. Acta Biochimica Polonica. 2020; 67: 465–473. https://doi.org/10.18388/abp.2020_5384.

[35] Meléndez-Fernández OH, Liu JA, Nelson RJ. Circadian Rhythms Disrupted by Light at Night and Mistimed Food Intake Alter Hormonal Rhythms and Metabolism. International Journal of Molecular Sciences. 2023; 24: 3392. https://doi.org/10.3390/ijms24043392.

[36] Lal H, Verma SK, Wang Y, Xie M, Young ME. Circadian Rhythms in Cardiovascular Metabolism. Circulation Research. 2024; 134: 635–658. https://doi.org/10.1161/CIRCRESAHA.123.323520.

[37] Ma J, Li Y, Yang X, Liu K, Zhang X, Zuo X, *et al*. Signaling pathways in vascular function and hypertension: molecular mechanisms and therapeutic interventions. Signal Transduction and Targeted Therapy. 2023; 8: 168. https://doi.org/10.1038/s41392-023-01430-7.

[38] Mulder JWCM, Kusters DM, Roeters van Lennep JE, Hutten BA. Lipid metabolism during pregnancy: consequences for mother and child. Current Opinion in Lipidology. 2024; 35: 133–140. https://doi.org/10.1097/MOL.0000000000000927.

[39] Admati I, Skarbianskis N, Hochgerner H, Ophir O, Weiner Z, Yagel S, *et al*. Two distinct molecular faces of preeclampsia revealed by single-cell transcriptomics. Med (New York, N.Y.). 2023; 4: 687–709.e7. https://doi.org/10.1016/j.medj.2023.07.005.

[40] Hosking SL, Moldenhauer LM, Tran HM, Chan HY, Groome HM, Lovell EA, *et al*. Treg cells promote decidual vascular remodeling and modulate uterine NK cells in pregnant mice. JCI Insight. 2024; 10: e169836. https://doi.org/10.1172/jci.insight.169836.

[41] Zhang X, Wei H. Role of Decidual Natural Killer Cells in Human Pregnancy and Related Pregnancy Complications. Frontiers in Immunology. 2021; 12: 728291. https://doi.org/10.3389/fimmu.2021.728291.